Novel function of STAT1β in B cells: induction of cell death by a mechanism different from that of STAT1α

Imen Najjar,*,[1] Pierre Olivier Schischmanoff,* Fanny Baran-Marszak,* Pierre-Antoine Deglesne,* Ibtissam Youlyouz-Marfak,† Mathieu Pampin,‡ Jean Feuillard,† Georg W. Bornkamm,§ Mounira K. Chelbi-Alix,‡ and Remi Fagard*,[2]

*Université Paris 13, EA 3406, Service de biochimie, APHP, Hôpital Avicenne, Cedex, France; ‡CNRS FRE 2937, Institut Lwoff, Villejuif, France; †Unité Mixte de Recherche (UMR), Centre National de la Recherche Scientifique (CNRS) 6101, and Laboratoire d'Hématologie, Centre Hospitalier Universitaire (CHU) Dupuytren and Faculté de Médecine, Université de Limoges, France; and §Forschungszentrum für Umwelt und Gesundheit (GSF), Institute of Clinical Molecular Biology and Tumor Genetics, Munich, Germany

Abstract: Alternate splicing of STAT1 produces two isoforms: α, known as the active form, and β, previously shown to act as a dominant-negative factor. Most studies have dealt with STAT1α, showing its involvement in cell growth control and cell death. To examine the specific function of either isoform in cell death, a naturally STAT1-deficient human B cell line was transfected to express STAT1α or STAT1β. STAT1α, expressed alone, enhanced cell death, potentiated the fludarabine-induced apoptosis, and enhanced the nuclear location, the phosphorylation, and the transcriptional activity of p53. Unexpectedly, STAT1β, expressed alone, induced cell death through a mechanism that was independent of the nuclear function of p53. Indeed, in STAT1β-expressing B cells, p53 was stricktly cytoplasmic where it formed clusters, and there was no induction of the transcriptional activity of p53. These data reveal a novel role of STAT1β in programmed cell death, which is independent of p53. *J. Leukoc. Biol.* 84: 1604–1612; 2008.

Key Words: *B lymphocytes · p53 · fludarabine*

INTRODUCTION

STAT1 is the mediator of several biological responses following stimulation by growth factors and cytokines. It plays an important role in innate and adaptive immunity [1–3], in B cell growth control [4], and in tumor surveillance [5], as it may function as a tumor suppressor [6, 7] and is known to be involved in apoptotic [8] and probably also in nonapoptotic [9, 10] cell death. Alternate splicing of STAT1 produces two isoforms: The long form, STAT1α, carries two phosphorylation sites, tyrosine 701 and serine 727, and a C-terminal transactivation domain (TAD), which recruits histone acetyltransferases and other coactivators [11], conferring maximal activity [12]. The short form, STAT1β, is expressed at a low level, and it lacks the TAD but is phosphorylated efficiently on tyrosine 701. Both isoforms can form homo (α/α or β/β)- and heterodimers (α/β), which bind to DNA [13–15]. The function of STAT1β is thought to be restricted to the inhibition of STAT1α, mainly as its overexpression can suppress specific STAT1α functions [15–17]. Yet, in the case of STAT3, it was found that STAT3β is not solely a physiologic dominant-negative of STAT3α but also has a unique and specific function [18]. Interestingly, the crucian carp expresses only the homologue of mammalian STAT1β (*Ca*STAT1), which activates the expression of IFN-dependent genes [19]. These studies point to the possibility of a specific function for the β isoform of STAT1.

Fludarabine, a purine analog, is incorporated into RNA and DNA, and it inhibits RNA synthesis and causes DNA damage [20, 21]. It is used in the treatment of solid tumors, lymphoma [22–24], and chronic lymphoid leukemia [25]. Activation of p53 is a critical step for the apoptotic response to fludarabine [26–28]. We previously found that p53 and STAT1α interact in apoptotic B cells following fludarabine treatment [15]. In addition, in cisplatin-treated, non-B cells, STAT1α was found to facilitate the phosphorylation of p53, to interact with it [29], and to potentiate its transcriptional activity [30]. This indicated that STAT1α regulates the p53 pathway. We also observed in a previous study that the overexpression of the β isoform of STAT1 in lymphoblastoid cell lines (LCLs), in which STAT1 is normally expressed, exerts a negative, inhibitory effect on this effector, resulting in the inhibition of the nuclear translocation of p53 and a protection of the cells against fludarabine-induced apoptosis [15]. These experiments, based on the notion that STAT1β is an inhibitor of STAT1α, demonstrated the involvement of STAT1α in fludarabine-induced apoptosis. Nevertheless, it remains to be clarified whether STAT1β alone can exert a function independently of its inhibitory role, a point that has never been explored in lymphoma cells. To investigate this, we restored the expression of STAT1β in a naturally STAT1-

[1] Current address: Institut Cochin, Inserm U567, 123 Bd de Port-Royal 75014, Paris, France.

[2] Correspondence: Service de biochimie, Hôpital Avicenne, 125 route de Stalingrad, 93009 Bobigny Cedex, France. E-mail: remi.fagard@avc.aphp.fr

Received May 5, 2008; revised July 23, 2008; accepted August 7, 2008.
doi: 10.1189/jlb.0508287

deficient (SD), human LCL [31] and observed that it induces cell death.

MATERIALS AND METHODS

Cell culture and treatments

The SD LCL (kindly provided by Stéphanie Boisson-Dupuis and Jean-Laurent Casanova, INSERM U550, France) and the control (Ct) LCL were grown at 37°C in a humidified, 5% CO_2 atmosphere at a density of 1×10^6 cells/ml in RPMI-1640 medium L-glutamine (Invitrogen, Carlsbad, CA, USA), supplemented, respectively, with 20% and 10% heat-inactivated FCS (PAN Biotech, Germany), 100 U/ml penicillin, and 10 μg/ml streptomycin (Gibco-BRL-Life Technologies, Gaithersburg, MD, USA). Where indicated, cells were treated with IFN-γ (Roche Diagnostics, Nutley, NJ, USA) or 9-β-D-arabinosyl-2-fluoroadenine (fludarabine, Schering-Plough, Kenilworth, NJ, USA) at the indicated concentrations. The TK6 (p53-proficient) and NH32 (p53-deficient) cells were a generous gift of Dr. Howard L. Liber (Department of Environmental and Radiological Health Sciences, Colorado State University, Fort Collins, CO, USA).

Plasmid constructs, transfections, and cell sorting

The STAT1α/nerve growth factor receptor (NGFR) and STAT1β/NGFR vectors were derived from the CKR 516 vector described previously [15]. These vectors contain a bidirectional tetracycline-inducible promoter driving the expression of two independent cDNAs—STAT1α or STAT1β—and a version of the NGFR lacking the cytoplasmic domain used as a marker of induction. Transfection, selection of hygromycin-resistant cells, and doxycycline induction were performed as described previously [15]. We performed control experiments to verify that the expression of the truncated NGFR itself was neutral. The SD cells were transfected with the episomally replicating pINCO/NGFR vector described previously [32]. The truncated NGFR sequence placed under the control of the cytomegalovirus promoter was identical to that of the CKR 516 vector. Sorting of the STAT1α/NGFR, STAT1β/NGFR, and NGFR-expressing cells was performed by magnetic separation using the MACSelect L-NGFR system following the manufacturer's protocol (Miltenyi Biotec, Auburn, CA, USA). NGFR-negative, sorted cells were used as an internal control for the effects of hygromicine selection, tetracycline treatment, and sorting procedure. The induction of the expression of NGFR on sorted cells was verified by flow cytometry, and the induction of the expression of STAT1α or STAT1β was assessed by Western blotting.

Western blot analysis

Cells were washed in PBS (bioMérieux, France), lysed in a denaturating sample buffer [50 mM Tris-HCl, pH 6.8 (Bio-Rad, Hercules, CA, USA), 2% SDS (Sigma Chemical Co., St. Louis, MO, USA), 20% glycerol (Prolabo), 1 mM $NaVO_3$ (Labosi), and 5% 2-ME (Merck, Rahway, NJ, USA)], supplemented with 0.01% bromophenol blue (Sigma Chemical Co.). The lysates were sonicated, boiled for 5 min, and stored at −80°C. Approximately 30 μg protein was separated on a 10% SDS-PAGE gel and transferred onto nitrocellulose membranes (Schleicher & Schuell, Germany). After transfer, the membranes were blocked for 1 h with 5% dry skimmed milk (Régilait, France) in TBS [20 mM NaCl (Sigma Chemical Co.), 500 mM Tris-HCl, pH 8 (Euromedex, France)]. The incubation with the first antibody was performed overnight in TBS at 4°C. The antibodies used were antiphosphotyrosine 701-STAT1 (Cell Signaling Technology, Beverly, MA, USA) at 1/1000, antiphosphoserine 727-STAT1 (Upstate Biotechnology, Lake Placid, NY, USA) at 1/1000, anti-STAT1 (Cell Signaling Technology) at 1/1000, anticleaved polyADP ribose polymerase (PARP; Cell Signaling Technology) at 1/1000, antiphosphoserine 20-p53 (Cell Signaling Technology) at 1/1000, antiphosphoserine 15-p53 (Cell Signaling Technology) at 1/1000, anti-p53 (D07; a generous gift of Dr. Evelyne May) at 1/20,000, and anti-actin (Santa Cruz Biotechnology, Santa Cruz, CA, USA) at 1/1000.

Blots were washed three times for 5 min in TBST and then incubated for 1 h with the appropriate peroxidase-coupled secondary antibody at 1/5000: goat anti-mouse (Santa Cruz Biotechnology), goat anti-rabbit (Upstate Biotechnology), or rabbit anti-goat (Sigma Chemical Co.). After three washes in TBST, blots were revealed by chemiluminescence (LumiGLO reagent and peroxide, Cell Signaling Technology) and autoradiography (X-Omat R film, Kodak, Rochester, NY, USA). When necessary, membranes were stripped and reprobed. For membranes stripping, the blot restore kit was used (Chemicon International, Temecula, CA, USA) following the manufacturer's protocol, and membranes were blotted and revealed as described above. To determine the molecular weight of proteins, prestained molecular weight standards (Fermentas, Glen Burnie, MD, USA) were used.

Flow cytometry

To determine the induction of NGFR by doxycycline, the binding of a PE-labeled NGFR antibody (NGFR-PE; Miltenyi Biotec) was measured by flow cytometry. To detect the early onset of apoptosis, we used the annexin V-FITC Apoptosis Detection Kit I (BD PharMingen, San Diego, CA, USA) or the MitoProbe JC-1 Assay Kit (Molecular Probes, Eugene, OR, USA). The chemical JC-1 (5,5′,6,6′-tetrachloro-1,1′,3,3′-tetrachloro-1,1′,3,3′-tetratylbenzimidazol carbocyanine iodide) emits a green fluorescence when it is free in the cytoplasm in monomeric form and a red fluorescence when it is bound to the intact mitochondria in dimeric form. In viable cells, the probe is red and green, but when cells undergo mitochondria-dependent apoptosis, the loss of mitochondrial transmembrane potential results in the loss of the red fluorescence and a decreased red/green ratio, reflecting cell death [33, 34]. For the labeling, 1×10^4 cells in 100 μl culture medium supplemented with FCS were incubated with 2 μM JC-1 for 20 min at 37°C in a humidified, 5% CO_2 atmosphere. Analysis of cell cycle was performed as described [15]; briefly, cells were fixed in 70% ethanol, then incubated in HCl 2 N, pepsin 0.2 mg/ml for 30 min, neutralized with $Na_2B_4O_7$, resuspended in PBS containing 0.1% Triton X100 (Sigma Chemical Co.) and 0.1 mg/ml RNase (Sigma Chemical Co.), incubated with anti-BrdU-FITC (BD PharMingen) for 30 min, and analyzed. The flow cytometry analyses were performed using a XL Beckman-Coulter counter.

Real-time quantitative PCR (qPCR)

Experiments were conducted using the TaqMan Gene Expression Cells-to-Ct Kit (Applied Biosystems, Foster City, CA, USA). SD cells, transfected or not with STAT1-α- or STAT1-β-expressing plasmids, were counted and washed in cold PBS. For each suspension of cells, four to five serial dilutions in fivefold increments were made to obtain 125,000, 25,000, 5000, 1000, and 200 cells in 5 μl. Each preparation (5 μl) was lysed, and 10 μl of each cell lysate was used for RT. For the amplification, the following TaqMan gene expression assays (Applied Biosystems) were used: p21Cip1/Waf1 (ref. Hs 99999142_m1), MDM2 (ref. Hs 01066930_m1), Bax (Hs 99999001_m1), and Cyclophilin A (PPIA; ref. Hs 99999904_m1). All assays were designed to amplify exon junctions and therefore, only detected cDNA templates. cDNA (5 μl), corresponding to each cell suspension, was mixed with TaqMan gene expression master mix and Taqman Gene expression assay in a final volume of 25 μl. The PCR conditions were: incubation for 2 min at 50°C, followed by an incubation for 10 min at 95°C, 40 cycles (denaturation step: 15 s at 95°C; annealing/elongation step: 60 s at 60°C), using a Taqman 7400 (Applied Biosystems). All steps were performed following the recommendations of the manufacturer. For each gene, the average cycle threshold (Ct) was plotted as a function of the logarithm of the cell number per lysis reaction. The values were linear from 75,000 to 200 cells per lysis reaction. Only the ΔCts (Ct of the gene studied–Ct Cyclophilin A), which remained unchanged independently of the cell number, were used to calculate the mean relative expression levels of each gene.

Immunofluorescence

Approximately 80,000 cells were centrifuged onto coverslips for 5 min at 800 rpm, dried for 5 min, fixed in 4% paraformaldehyde for 20 min at 4°C, and washed three times with PBS. The coverslips were then incubated 45 min at 37°C with anti-p53 (D07; similar results were obtained with D01, Santa Cruz Biotechnology) at 1/50 and antiphosphotyrosine 701 STAT1α/β (Cell Signaling Technology) at 1/100. After three washes in PBS-0.1% Tween (PBS-T), the coverslips were incubated with Alexa Fluor 594 rabbit anti-mouse IgG (Molecular Probes) and Alexa Fluor 488 goat anti-rabbit IgG (A11034, Molecular Probes) at 1/400 and 1/1000, respectively. After 45 min at 37°C, the coverslips

were washed three times in PBS-T, and nuclei were counterstained with 4′,6-diamidino-2-phenylindole, dihydrochloride (DAPI; Molecular Probes) at 1/250. After three washes with PBS-T, the coverslips were mounted using DAKO fluorescent mounting medium (DakoCytomation, Denmark). Images were obtained by confocal laser scanning on a Leica TCS-NT/SP. Z series were generated by collecting a stack consisting of eight to 10 optical sections using a step size of 0.3 μ in the Z direction. Images were processed using the Zeiss LSM image browser.

RESULTS

The SD B cells are less sensitive than the control B cells to fludarabine-induced apoptosis

In the Ct LCL, STAT1 was expressed and constitutively phosphorylated on the tyrosine 701 and the serine 727, as we and others [35–37] showed previously, and it was undetectable in the SD LCL (**Fig. 1A**). To study the function of STAT1 in apoptotic cell death and cell cycle, we exposed the cells to different concentrations of fludarabine, following which double annexin V-FITC/propidium iodide (PI) staining, JC-1 staining, PARP cleavage, and cell cycle were analyzed. We observed that in Ct LCL, there was a clear, concentration-dependent induction of apoptosis and reduction of viability by fludarabine, and in SD LCL, there was almost no change, except for a slight activation at 50 μM fludarabine (Fig. 1, B–D). The cell cycle was inhibited markedly in SD LCL treated with 5 μM fludarabine (S-phase at 10.5%) but not in Ct LCL (S-phase at 30%), and there was less difference at higher concentrations of fludarabine (25 and 50 μM; Fig. 1E). Thus, in the absence of STAT1, the B cells are somewhat protected against fludarabine-induced apoptosis, possibly because of a cell cycle arrest. We next compared the sensitivity to fludarabine (25 μM) of the SD B cells with that of LCL expressing wild-type (TK6) or inactivated (NH32) p53 [38]. Cell death induction by fludarabine, which was maximal in the TK6 cells, was completely suppressed in the NH32 cells, as shown previously [38]; interestingly, in the SD LCL (SD and p53-proficient), there was almost no induction of cell death by fludarabine (**Fig. 2A**). We also verified that in lymphoblastoid cells that were STAT1-proficient, there was little effect of IFN-γ treatment on cell growth or cell death; although interestingly, in fludarabine-treated cells, the addition of IFN-γ increased the number of cells in S-phase (threefold, Fig. 2B, Panel 4) and simultaneously increased somewhat the number of cells in sub-G1 (30%, Fig. 2B, Panel 4). This suggests a complex role of activated STAT1. The regulation underlying this process may rely in part on the level of expression of STAT1. The effect of IFN-γ on fludarabine-treated cells indicates that STAT1 acts, in this context, on cell cycle progress.

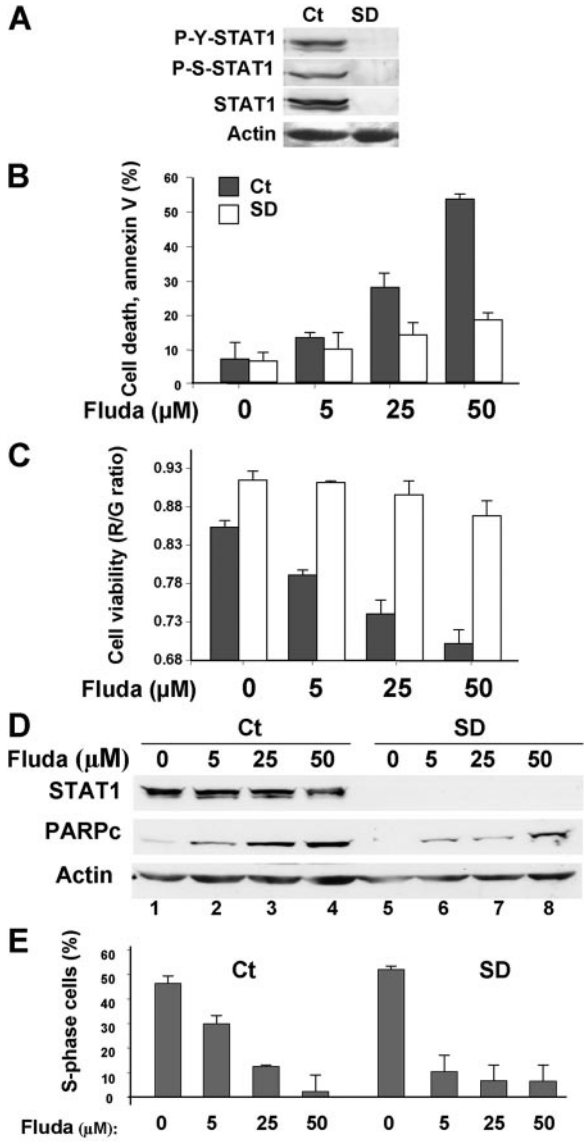

Fig. 1. SD B cells are resistant to fludarabine-induced apoptosis. (A) Expression and phosphorylation of STAT1α and STAT1β in Ct and SD LCLs were assessed by Western blotting using antiphosphotyrosine 701 STAT1 (P-Y-STAT1), antiphosphoserine 727 STAT1 (P-S-STAT1), and anti-STAT1α/β antibodies; actin was used as a loading control. (B) Cells were treated with increasing concentrations of fludarabine (Fluda) for 20 h, and apoptosis was analyzed by annexin V binding. (C) Cells were treated as in B, and their viability was measured by JC-1 staining (the quantification of the red/green fluorescence ratio is shown). Experiments were repeated three times. (D) Cells were treated as in B, and Western blotting with an anticleaved PARP (PARPc) antibody was performed; a typical result is shown. (E) Analysis of the fludarabine-induced cell cycle arrest in Ct and SD LCLs. The cell cycle was analyzed by flow cytometry after BrdU incorporation with the same cells as in B. The histograms represent the percentages of cells in the S-phase. This experiment was repeated three times.

Restoring the expression of STAT1α and STAT1β in B cells

To investigate the role of STAT1 in fludarabine-induced cell death, we transfected the SD LCL with episomal-inducible and bidirectionnal NGFR/STAT1α or NGFR/STAT1β vectors. Stable cell lines expressing STAT1α (SD-α) or STAT1β (SD-β) were obtained by magnetic selection using anti-NGFR coupled to magnetic microbeads. As a result of the constitutive IFN production by LCLs [37], 701 tyrosine residue and 727 serine residue were constitutively phosphorylated in SD-α cells (**Fig. 3**, Lane 5), but because of the C-terminal truncation, only tyrosine 701 was phosphorylated in SD-β cells (Fig. 3, Lane 7). We verified that the phosphorylation of the α and the β

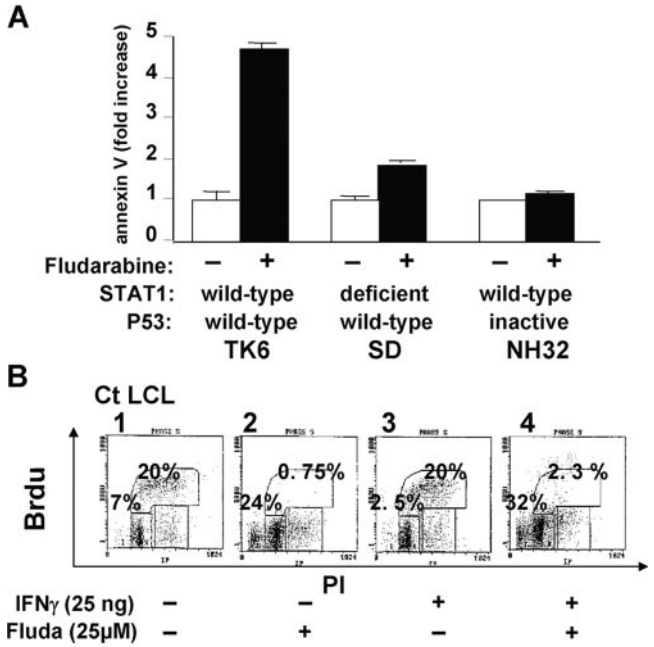

Fig. 2. Cell cycle arrest and cell death are reduced in p53-deficient and in SD cells. (A) Three cell types were compared for their sensitivity to 25 μM fludarabine: the TK6 cell line with functional p53 and STAT1, the SD cell line with functional p53 but nonfunctional STAT1, and the NH32 cell line with nonfunctional p53 and functional STAT1. The cells with nonfunctional p53 are insensitive to concentrations of fludarabine, which induce cell death in the TK6 cells. In the SD cells, the situation is intermediate, suggesting that STAT1 is required for optimal functionning of p53. Experiments were repeated three times. (B) Cell cycle progression was determined by measuring the incorporation of PI and BrdU in cells, followed by cytometry. In the Ct LCL (used in Fig. 1), fludarabine (25 μM) blocks cell division (Panel 2, 0.75% of cells in S-phase). After IFN-γ treatment of fludarabine-treated cells, there is an increase of cells in S-phase to 2.3% (Panel 4) and a 30% increase in cells in sub-G1 peak (Panel 4). Panel 1 shows untreated cells, and Panel 3 shows IFN-γ-treated cells.

isoforms was increased following addition of IFN-γ (Fig. 3, Lanes 6 and 8).

Restoration of STAT1α induces apoptosis and potentiates fludarabine-induced apoptosis of B cells

To examine the role of STAT1α in cell death, stable, transfected SD-α/NGFR cells were used. They were induced with doxycycline and sorted to obtain SD-α/NGFR-positive and -negative homogeneous cell populations. More than 84% of the negative-sorted SD-α cells were viable, exhibiting a red and green JC-1 fluorescence (**Fig. 4A**, SD-α, NGFR–), which was practically identical to that observed in nontransfected and untreated SD cells. Thus, a high red/green ratio: 0.9 ± 0.05 (Fig. 4B, SD-α, NGFR–) was found for the SD-α/NGFR-negative, sorted population, indicating that the cells were viable and that sorting did not affect the viability; in addition, in an independent experiment using SD cells transfected with the pINCO/NGFR vector, we confirmed that the expression of the truncated NGFR and cell sorting had no effect on cellular viability of our B cells (note that in subsequent experiments, the Ct cells are SD cells, and the SD-α/NGFR+ sorted cells are simply designated SD-α). Thus, in the SD-α cells, the red fluorescence of JC-1 was reduced markedly with the appearance of a peak of cells with negative red fluorescence (Fig. 4A, SD-α, NGFR+, see arrow), resulting in a decrease of the red/green ratio, indicating reduced cell viability (Fig. 4B). When stained with annexin V-FITC/PI, 44% of the SD-α cells were annexin V-positive (33% annexin V+/PI– and 11% annexin V+/PI+; see Fig. 5A, untreated SD-α). Thus, clearly, the restoration of STAT1α expression in SD cells induces cell death.

We then asked whether SD-α cells recovered their sensitivity to fludarabine. We observed that 74% of the fludarabine-treated SD-α cells were positive for annexin V binding (of which, 53% were PI–, and 21% were PI+; **Fig. 5, A**, upper panel SD-α, and **B**) and that the red/green ratio of JC-1 fluorescence was reduced following fludarabine treatment (Fig. 5A, SD-α for the corresponding graphs; see Fig. 5C). These data demonstrate that STAT1α sensitizes cells to fludarabine-induced cell death. In addition, we observed an increased cleavage of PARP in treated SD-α cells (Fig. 5D, Lane 2), showing that they undergo an apoptotic type of cell death following fludarabine treatment. These results demonstrate further that STAT1α plays an important role in the molecular mechanims triggered by fludarabine and raise the question of the function of the β isoform.

Restoration of STAT1β in B cells induces cell death, but the fludarabine-induced apoptosis is no longer detectable

We reintroduced STAT1β in the SD cells and studied its implication in cell death. Stable, transfected SD-β/NGFR cells were induced with doxycycline and sorted to obtain SD-β/NGFR-positive and -negative, homogeneous cell populations. As mentioned above, the cellular sorting did not affect cell viability, as in sorted, NGFR-negative populations, more than 81% of the cells were viable, exhibiting red and green JC-1 fluorescence (see Fig. 4A, SD-β, NGFR–), resulting in an elevated red/green ratio: 0.88 ± 0.05 (see Fig. 4B, SD-β, NGFR–). In SD-β/NGFR-positive, sorted cells (referred to in the following experiments as SD-β), 50% of the cells had lost the JC-1 red fluorescence, resulting in a peak of red-negative,

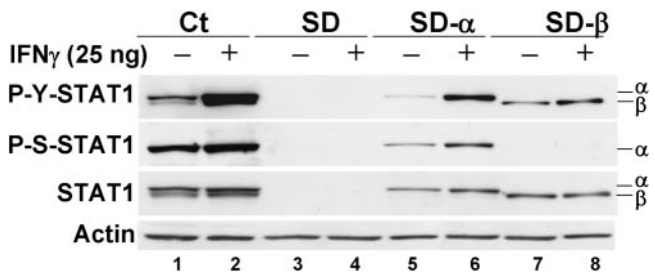

Fig. 3. Restoration of STAT1α or STAT1β. The SD LCL was stably transfected with the STAT1α/NGFR or the STAT1β/NGFR plasmid. STAT1α and -β expressions were induced by treating cells with 0.8 μg/ml doxycycline for 24 h, and cells were selected using magnetic microbead-coupled anti-NGFR. Ct, SD, and STAT1α-expressing (SD-α) and STAT1β-expressing (SD-β) LCLs were treated or not with IFN-γ (25 ng/ml). Cells were lysed, and expression and phosphorylation of STAT1α and/or STAT1β were assessed by Western blotting.

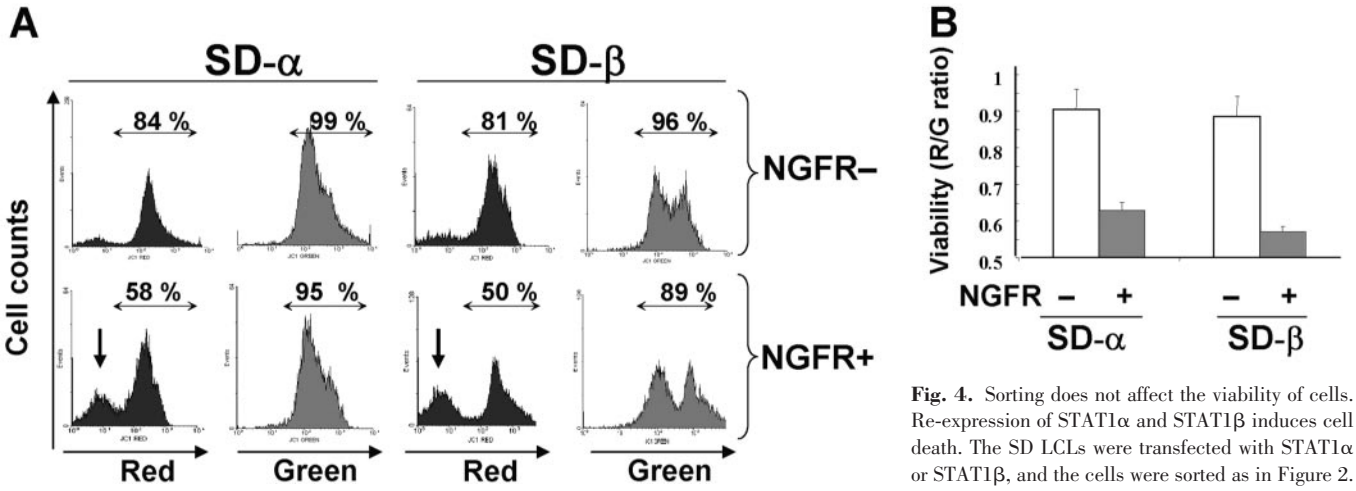

Fig. 4. Sorting does not affect the viability of cells. Re-expression of STAT1α and STAT1β induces cell death. The SD LCLs were transfected with STAT1α or STAT1β, and the cells were sorted as in Figure 2. Sorted-negative (NGFR–) and -positive (NGFR+) SD-α and SD-β cells were recovered. (A) Cellular sorting did not affect the viability and STAT1α- and STAT1β-induced cell death. NGFR– and NGFR+ cells were incubated with 2 μM JC-1 for 20 min at 37°C, and stained cells were analyzed by flow cytometry. (B) Histograms of the red/green fluorescence ratio (R/G) of JC-1 extracted from several experiments as in A.

fluorescent SD-β cells (Fig. 4A, SD-β, NGFR+, see arrow), which led to a decrease of the red/green ratio, indicating reduced cell viability (Fig. 4B, SD-β, NGFR+). In addition, 78% of the SD-β cells were annexin V-positive (almost twice the amount observed with SD-α cells; see Fig. 5A, untreated SD-β). These data reveal for the first time that when expressed in the absence of STAT1α, STAT1β is an inducer of cell death.

We next analyzed the response of SD-β cells to fludarabine treatment. Surprisingly, there was no significant difference in cell death induction between fludarabine-treated and nontreated SD-β cells: The percentage of annexin V-positive cells (Fig. 5, A, SD-β, and B), the red/green ratio of JC-1 fluorescence (Fig. 5C, SD-β), and the level of cleaved PARP (Fig. 5D, Lane 4) did not change following fludarabine treatment. This demonstrates that STAT1β is able to induce a high cell death, but unlike STAT1α, it does not allow enhanced, fludarabine-induced apoptotic cell death.

The p53 pathway has been shown to play a major role in fludarabine-induced apoptosis, and as shown above (see Fig. 2A), the effect of the absence of expression of STAT1 on cell death is somewhat reminiscent of the absence or inactivation of p53. We therefore studied the p53 status in B cells that were transfected with STAT1α or STAT1β.

STAT1β, unlike STAT1α, does not allow nuclear translocation or transcriptional activation of p53

The p53 pathway is one of the major molecular mechanisms mediating fludarabine cytotoxicity [28, 39] and involves STAT1α [15, 40]. However, whether STAT1β is involved has not been elucidated. Phosphorylation of the amino terminal domain of p53, particularly of serine 15 and 20, plays an important role in its activation, stabilization, and transcriptional activity [41]. We observed that the level of p53 and its phosphorylation on serine 15 were increased in Ct LCL following treatment with fludarabine (**Fig. 6A**, Lanes 1–4). In SD LCL, the level of p53 and its phosphorylation on serine 15 were lower at those concentrations (Fig. 6A, Lanes 5–8), in accordance with their reduced sensitivity to fludarabine-induced apoptosis (see Fig. 1B). By contrast, at 50 μM fludarabine, the phosphorylation of serine 20 occurred only with STAT1α and was much less pronounced with STAT1β, and the phosphorylation of serine 15 was almost similar (Fig. 6B). Thus, in the presence of STAT1α, the phosphorylation of serine 20 of p53 was enhanced after fludarabine treatment, whereas in the presence of STAT1β, no change occurred. To further analyze the effect of STAT1β on p53, we examined the subcellular location in SD-α and SD-β LCLs. We found that in SD LCL, the nuclear location observed for p53 following fludarabine treatment in SD LCL was reduced as compared with Ct LCL (**Fig. 7A**). In nontreated SD-α, p53 was present in the nucleus, but upon fludarabine treatment, more p53 became nuclear (Fig. 7A). However, in the SD-β LCL, p53 was practically not detected in the nucleus of untreated cells and not at all in the nucleus of fludarabine-treated cells; instead, p53 was forming aggregates in the cytoplasm (Fig. 7A). To explore the transcriptional activity of p53, we studied the expression of its targets p21WAF1, hMdm2, and Bax by real-time-PCR in STAT1α- or STAT1-β-transfected SD cells. We found that compared with Ct SD LCLs, the expression of p21WAF1, hMdm2, and Bax was increased in the SD-α LCLs and diminished in the SD-β LCLs (Fig. 7B). Thus, the results indicate that the induction of cell death by STAT1β is independent of the nuclear location of p53; this is corroborated by the absence of induction of the p53 targets in the SD-β LCLs.

STAT1β, as opposed to STAT1α, does not interact with p53 in B cells following fludarabine treatment

Following treatment of cells with chemotoxic agents, STAT1α and p53 have been found previously associated by a direct interaction [15, 40]. Here, we analyzed the interaction of p53 and STAT1 in cells that were treated or not with fludarabine. Using confocal microscopy, we observed a diffuse cytoplasmic location of STAT1α and p53 in untreated SD-α cells; this cytoplasmic labeling was enhanced by fludarabine treatment, and as in Figure 7A, p53 became detectable in the nucleus. In

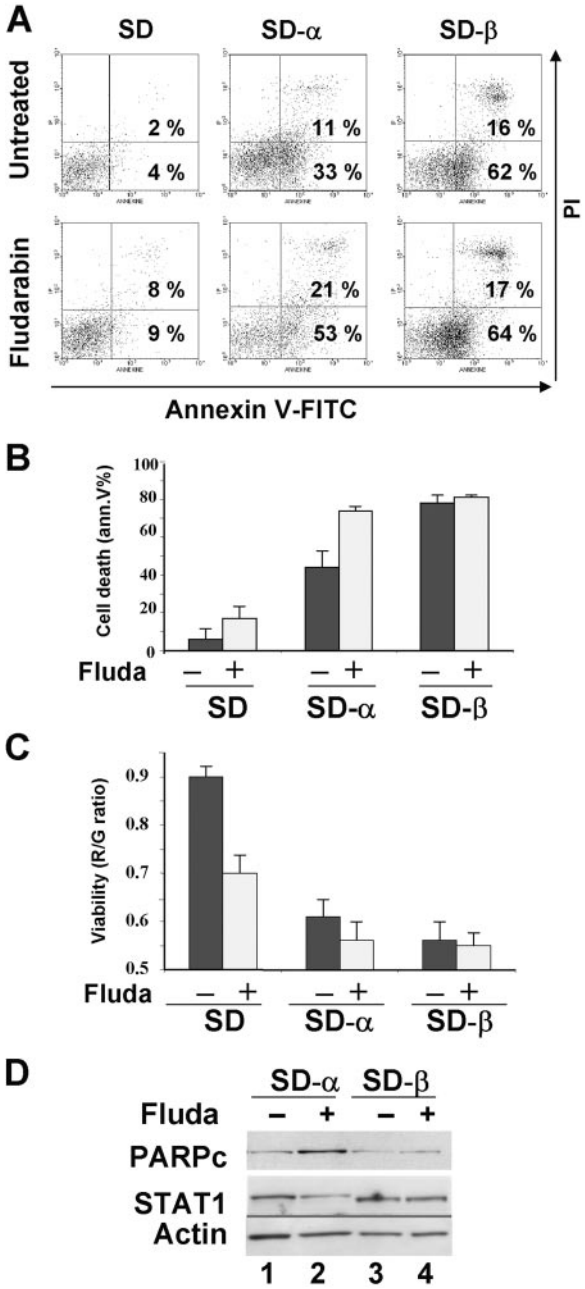

Fig. 5. STAT1α- and STAT1β-transfected LCLs respond differently to fludarabine treatment. Analysis of the fludarabine-induced apoptosis in SD, SD-α, and SD-β cells, which were treated with fludarabine for 20 h. (A) SD LCL and positive NGFR+ sorted SD-α and SD-β LCLs were treated or not with 50 μM fludarabine for 20 h and analyzed for annexin V binding and PI staining by flow cytometry. (B) Comparative quantitative histograms of experiments performed with SD, SD-α, and SD-β cells, as shown in A, and a typical experiment is shown. (C) Comparative quantitative histograms of experiments with SD, SD-α, and SD-β cells treated or not with 50 μM fludarabine and stained by JC-1; after 20 h of treatment, the percentage of cells exhibiting red- and green-positive fluorescence was quantified by flow cytometry. The red/green fluorescence ratio is shown. The experiments were repeated three times. (D) Differential induction of PARP cleavage following STAT1α or -β transfection: Cells were lysed and Western blotting performed using anti-cleaved PARP and anti-STAT1α/β antibodies. Actin was used to control equal loading. The experiments were repeated several times. A typical representative experiment is shown.

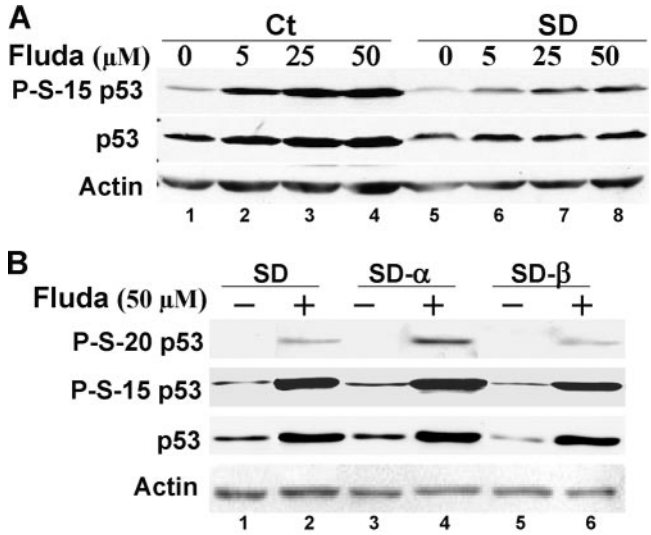

Fig. 6. Differential modulation of the phosphorylation of p53. (A) Ct and SD LCLs were treated for 20 h with increasing concentrations of fludarabine, total cellular proteins were obtained, and expression of p53 and its phosphorylation on serine 15 (P-S-15 p53) was analyzed by Western blotting. (B) SD and sorted-positive SD-α and SD-β LCLs were treated for 20 h with 50 μM fludarabine, and expression of p53 and its phosphorylation on serine 15 and serine 20 was analyzed by Western blotting. Actin was used as a control of equal loading.

addition, the yellow color of the overlay suggested colocation of STAT1α and p53 (**Fig. 8**). By contrast, in SD-β cells, STAT1β and p53 were detected in completely distinct areas of the cytoplasm, and similar to what we observed in Figure 7A, p53 was practically undetectable in the nucleus of fludarabine-treated SD-β cells (Fig. 8). These confocal microscopy images suggest a major difference between SD-α and SD-β in their ability to form complexes with p53 following fludarabine treatment. Indeed, we found that as previously demonstrated [29], STAT1α and p53 coimmunoprecipitated, but STAT1β and p53 did not (not shown). Taken together, these data show that unlike STAT1α, in the cellular context of LCL, STAT1β cannot form a complex with p53.

DISCUSSION

In this paper, we find that the absence of STAT1 in human B cells confers resistance to DNA damaging compounds such as fludarabine. Restoration of the STAT1 isoforms does not have similar effects: The α isoform cooperates with p53 and restores the sensitivity to fludarabine, but the β isoform induces cell death by itself in a manner that is independent of p53.

STAT1 has been known for some time to be a key element in the regulation of the cell death machinery in response to several stimuli. Indeed, we find here in the SD B cells that the apoptotic response to cytotoxic agents (such as fludarabine) is impaired, confirming data obtained in fibroblasts by other laboratories [29]. Paradoxically, in our experiments, the addition of fludarabine to SD cells inhibited cell cycle progression, suggesting that STAT1 modulates the expression of a subset of p53 target genes that are specifically involved in this process.

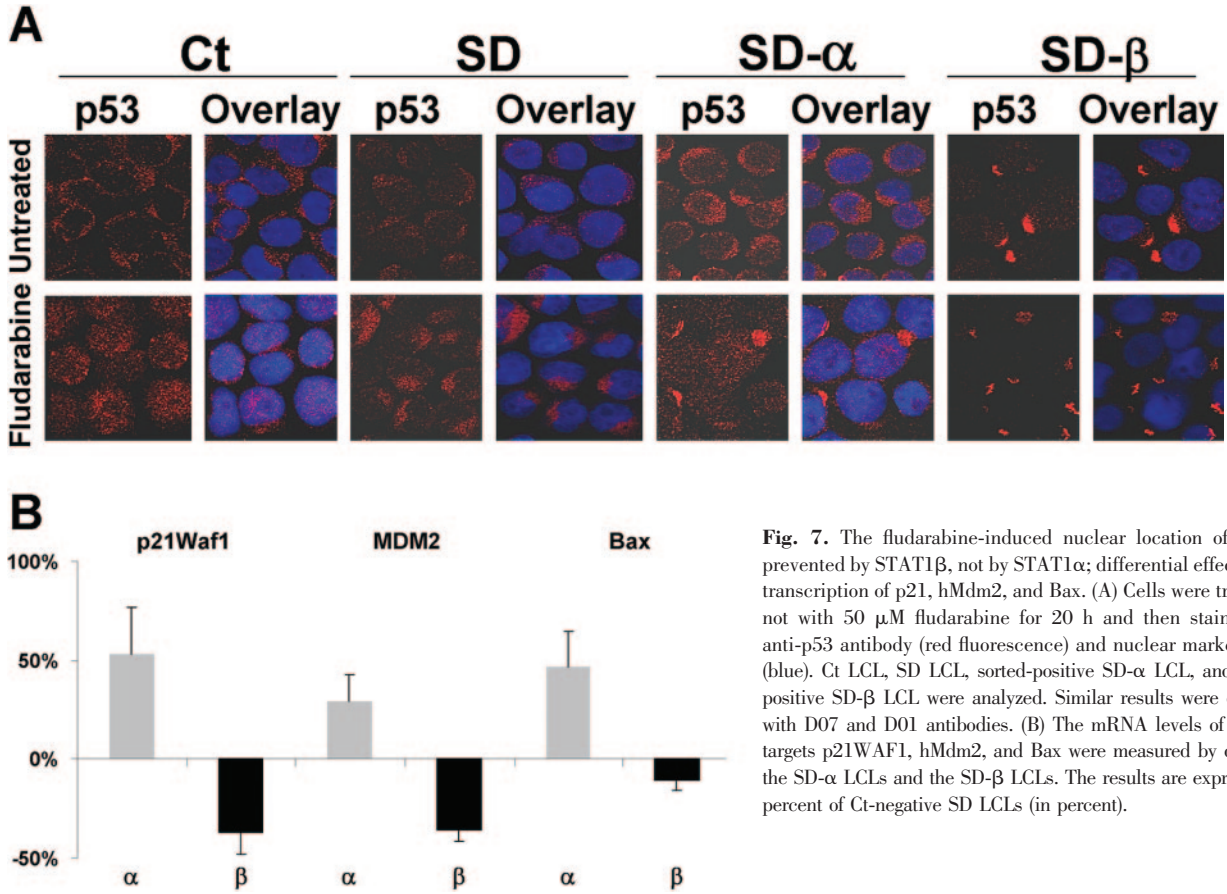

Fig. 7. The fludarabine-induced nuclear location of p53 is prevented by STAT1β, not by STAT1α; differential effect on the transcription of p21, hMdm2, and Bax. (A) Cells were treated or not with 50 μM fludarabine for 20 h and then stained with anti-p53 antibody (red fluorescence) and nuclear marker DAPI (blue). Ct LCL, SD LCL, sorted-positive SD-α LCL, and sorted-positive SD-β LCL were analyzed. Similar results were obtained with D07 and D01 antibodies. (B) The mRNA levels of the p53 targets p21WAF1, hMdm2, and Bax were measured by qPCR in the SD-α LCLs and the SD-β LCLs. The results are expressed as percent of Ct-negative SD LCLs (in percent).

The α isoform is classically considered to be the physiologically active form, and the β isoform is considered to be its physiological inhibitor. Indeed, our previous results show that overexpression of STAT1β inhibits STAT1α, resulting in a protection of the B cells from fludarabine-induced apoptosis [15]. In line with this view is the demonstration that *Mycobacterium avium intracellularae* and *Leishmania mexicana* can overcome the IFN-γ-triggered host cell defense by inducing STAT1β, thereby inhibiting STAT1α [16, 17]. Thus, these observations made in different contexts are in favor of a STAT1α-inhibitory function for STAT1β. On the other hand, the fact that in the carp, a STAT1β homologue is sufficient for an IFN response to viral infection [19] pointed to a specific function of STAT1β. One possibility to study the β isoform individually was to specifically block the expression of the α isoform by using small interfering RNA, but this method did not really achieve a complete suppression of the expression in our cell system. In humans, STAT1 deficiency has been rarely observed; thus, experiments with SD cells are limited to cell lines that were derived from SD patients [31, 42].

Restoring STAT1 expression in SD cells has the key advantage that one does not have to inhibit this factor, avoiding the drawback of incomplete inhibition. Still, the SD cells may harbor modifications that compensate for the absence of STAT1 and that could interfere with it once it is reintroduced. Apart from this possibility, our experimental system provided a unique opportunity to search for a function for STAT1β in B cells. Indeed, reintroduction of STAT1β showed that it can function in the absence of the α isoform; however, its precise mechanism of action is not known. Contrary to STAT3β, which was found to have targets [18] and although STAT1α was found to form complexes with other transcription factors such as NF-κB [43] or specificity protein 1 [44], STAT1β does not have a clearly identified transcriptional activity [14, 45]. Thus, whether the unique behavior of STAT1β results from distinct transcriptional targets is not clear. Although induction of cell death was clearly the result of the expression of STAT1β, it could result from modulation of other factors involved in cell death.

The cell death observed upon restoration of the expression of STAT1α and treatment by fludarabine had the characteristics of apoptosis: PARP cleavage and annexin V binding. On the other hand, upon restoration of STAT1β, PARP cleavage and annexin V binding were not increased significantly by fludarabine treatment. More challenging was the modification of the subcellular location of p53 following STAT1β induction. p53 is known to be activated and to translocate to the nucleus upon fludarabine treatment. p53 is thus considered to be a major component of the fludarabine-triggered apoptotic machinery. Indeed, in the SD-α cells, fludarabine induced a substantial transfer of p53 to the nucleus in agreement with a major function of this effector. The induction of the expression of STAT1β had a completely different effect on p53, and in particular, there was no detectable p53 in the nucleus. This indicates that there is no involvement of the nuclear activity of p53 in the cell death triggered by STAT1β. In fact, our immunofluorescence data suggest the presence of STAT1α/p53 complexes and a complete absence of any complex of STAT1β

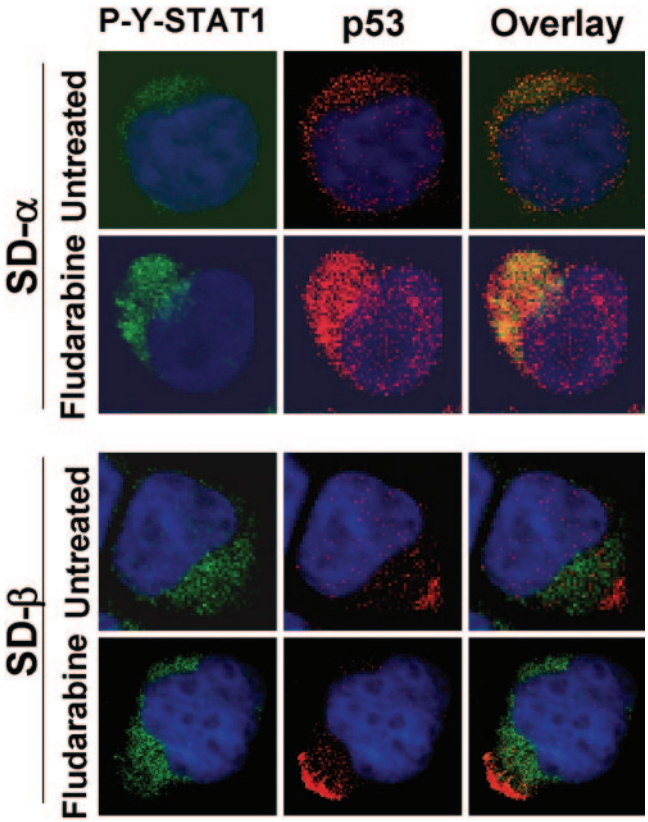

Fig. 8. Differential location of p53 and STAT1 in STAT1α- or -β-expressing B cells. SD and sorted-positive SD-α and SD-β LCLs were treated or not with 50 μM fludarabine for 20 h: cells were stained with anti-P-Y-STAT1 antibody (green fluorescence), anti-p53 antibody (red fluorescence), and nuclear marker DAPI (blue). Similar results were obtained with D07 and D01 antibodies.

with p53, in agreement with our previous results [15] and results from other laboratories [30]. In addition, in STAT1β-transfected SD LCLs, the subcellular location of p53 within the cytoplasm and the formation of aggregates were quite unusual. The presence of these aggregates containing p53 within the cytoplasm together with the notion that p53 is not found in the nucleus suggest that the STAT1β-induced cell death is different from that induced by STAT1α and is mediated by mechanisms that are unknown. Further work is needed to decipher the precise molecular mechanism involved.

In conclusion, we find that SD human B cells are somewhat protected against fludarabine-induced apoptosis. We show that although the restoration of STAT1α restores the sensitivity to fludarabine, the restoration of STAT1β is in itself sufficient to induce cell death in a manner that does not require a nuclear function of p53 and is independent of STAT1α.

ACKNOWLEDGMENTS

This work was supported in part by ARC, Grant No. 3133, and by a grant from the "réseau INSERM herpèsvirus et cancer." I. N. was supported by Ministère de l'Education Nationale, de la Recherche et des Technologies (MENRT) and Société Française d'Hématologie (SFH). We thank Stéphanie Boisson-Dupuis and Jean-Laurent Casanova for the gift of SD B cells, Howard Liber for the gift of TK6 and NH32 cells, and Evelyne May for the gift of D07 antibody.

REFERENCES

1. Durbin, J. E., Hackenmiller, R., Simon, M. C., Levy, D. E. (1996) Targeted disruption of the mouse Stat1 gene results in compromised innate immunity to viral disease. *Cell* **84,** 443–450.
2. Durbin, J. E., Fernandez-Sesma, A., Lee, C. K., Rao, T. D., Frey, A. B., Moran, T. M., Vukmanovic, S., Garcia-Sastre, A., Levy, D. E. (2000) Type I IFN modulates innate and specific antiviral immunity. *J. Immunol.* **164,** 4220–4228.
3. Dupuis, S., Dargemont, C., Fieschi, C., Thomassin, N., Rosenzweig, S., Harris, J., Holland, S. M., Schreiber, R. D., Casanova, J. L. (2001) Impairment of mycobacterial but not viral immunity by a germline human STAT1 mutation. *Science* **293,** 300–303.
4. Lee, C. K., Smith, E., Gimeno, R., Gertner, R., Levy, D. E. (2000) STAT1 affects lymphocyte survival and proliferation partially independent of its role downstream of IFN-γ. *J. Immunol.* **164,** 1286–1292.
5. Miller, D. M., Rahill, B. M., Boss, J. M., Lairmore, M. D., Durbin, J. E., Waldman, J. W., Sedmak, D. D. (1998) Human cytomegalovirus inhibits major histocompatibility complex class II expression by disruption of the Jak/Stat pathway. *J. Exp. Med.* **187,** 675–683.
6. Bromberg, J., Darnell Jr., J. E. (2000) The role of STATs in transcriptional control and their impact on cellular function. *Oncogene* **19,** 2468–2473.
7. Ouchi, T., Lee, S. W., Ouchi, M., Aaronson, S. A., Horvath, C. M. (2000) Collaboration of signal transducer and activator of transcription 1 (STAT1) and BRCA1 in differential regulation of IFN-γ target genes. *Proc. Natl. Acad. Sci. USA* **97,** 5208–5213.
8. Sironi, J. J., Ouchi, T. (2004) STAT1-induced apoptosis is mediated by caspases 2, 3, and 7. *J. Biol. Chem.* **279,** 4066–4074.
9. Xu, Y., Kim, S. O., Li, Y., Han, J. (2006) Autophagy contributes to caspase-independent macrophage cell death. *J. Biol. Chem.* **281,** 19179–19187.
10. Kim, H. S., Lee, M. S. (2005) Essential role of STAT1 in caspase-independent cell death of activated macrophages through the p38 mitogen-activated protein kinase/STAT1/reactive oxygen species pathway. *Mol. Cell. Biol.* **25,** 6821–6833.
11. Zhang, J. J., Zhao, Y., Chait, B. T., Lathem, W. W., Ritzi, M., Knippers, R., Darnell Jr., J. E. (1998) Ser727-dependent recruitment of MCM5 by Stat1α in IFN-γ-induced transcriptional activation. *EMBO J.* **17,** 6963–6971.
12. Wen, Z., Zhong, Z., Darnell Jr., J. E. (1995) Maximal activation of transcription by Stat1 and Stat3 requires both tyrosine and serine phosphorylation. *Cell* **82,** 241–250.
13. Vinkemeier, U., Cohen, S. L., Moarefi, I., Chait, B. T., Kuriyan, J., Darnell Jr., J. E. (1996) DNA binding of in vitro activated Stat1 α, Stat1 β and truncated Stat1: interaction between NH2-terminal domains stabilizes binding of two dimers to tandem DNA sites. *EMBO J.* **15,** 5616–5626.
14. Zakharova, N., Lymar, E. S., Yang, E., Malik, S., Zhang, J. J., Roeder, R. G., Darnell Jr., J. E. (2003) Distinct transcriptional activation functions of STAT1α and STAT1β on DNA and chromatin templates. *J. Biol. Chem.* **278,** 43067–43073.
15. Baran-Marszak, F., Feuillard, J., Najjar, I., Le Clorennec, C., Bechet, J. M., Dusanter-Fourt, I., Bornkamm, G. W., Raphael, M., Fagard, R. (2004) Differential roles of STAT1α and STAT1β in fludarabine-induced cell cycle arrest and apoptosis in human B cells. *Blood* **104,** 2475–2483.
16. Alvarez, G. R., Zwilling, B. S., Lafuse, W. P. (2003) *Mycobacterium avium* inhibition of IFN-γ signaling in mouse macrophages: Toll-like receptor 2 stimulation increases expression of dominant-negative STAT1 β by mRNA stabilization. *J. Immunol.* **171,** 6766–6773.
17. Bhardwaj, N., Rosas, L. E., Lafuse, W. P., Satoskar, A. R. (2005) Leishmania inhibits STAT1-mediated IFN-γ signaling in macrophages: increased tyrosine phosphorylation of dominant negative STAT1β by *Leishmania mexicana*. *Int. J. Parasitol.* **35,** 75–82.
18. Maritano, D., Sugrue, M. L., Tininini, S., Dewilde, S., Strobl, B., Fu, X., Murray-Tait, V., Chiarle, R., Poli, V. (2004) The STAT3 isoforms α and β have unique and specific functions. *Nat. Immunol.* **5,** 401–409.
19. Zhang, Y., Gui, J. (2004) Molecular characterization and IFN signal pathway analysis of *Carassius auratus* CaSTAT1 identified from the cultured cells in response to virus infection. *Dev. Comp. Immunol.* **28,** 211–227.

20. Huang, P., Plunkett, W. (1991) Action of 9-β-D-arabinofuranosyl-2-fluoroadenine on RNA metabolism. *Mol. Pharmacol.* **39,** 449–455.
21. Rao, V. A., Plunkett, W. (2003) Activation of a p53-mediated apoptotic pathway in quiescent lymphocytes after the inhibition of DNA repair by fludarabine. *Clin. Cancer Res.* **9,** 3204–3212.
22. Leiby, J. M., Snider, K. M., Kraut, E. H., Metz, E. N., Malspeis, L., Grever, M. R. (1987) Phase II trial of 9-β-D-arabinofuranosyl-2-fluoroadenine 5′-monophosphate in non-Hodgkin's lymphoma: prospective comparison of response with deoxycytidine kinase activity. *Cancer Res.* **47,** 2719–2722.
23. Leiby, J. M., Grever, M. R., Staubus, A. E., Neidhart, J. A., Malspeis, L. (1988) Phase I clinical investigation of fludarabine phosphate by a loading-dose and continuous-infusion schedule. *J. Natl. Cancer Inst.* **80,** 447–449.
24. Kavanagh, J. J., Stringer, C. A., Copeland, L. J., Gershenson, D. M., Saul, P. (1986) Phase II trial of fludarabine in patients with epithelial ovarian cancer. *Cancer Treat. Rep.* **70,** 425–426.
25. Keating, M. J., Kantarjian, H., Talpaz, M., Redman, J., Koller, C., Barlogie, B., Velasquez, W., Plunkett, W., Freireich, E. J., McCredie, K. B. (1989) Fludarabine: a new agent with major activity against chronic lymphocytic leukemia. *Blood* **74,** 19–25.
26. Wattel, E., Preudhomme, C., Hecquet, B., Vanrumbeke, M., Quesnel, B., Dervite, I., Morel, P., Fenaux, P. (1994) p53 mutations are associated with resistance to chemotherapy and short survival in hematologic malignancies. *Blood* **84,** 3148–3157.
27. Feng, L., Achanta, G., Pelicano, H., Zhang, W., Plunkett, W., Huang, P. (2000) Role of p53 in cellular response to anticancer nucleoside analog-induced DNA damage. *Int. J. Mol. Med.* **5,** 597–604.
28. Rosenwald, A., Chuang, E. Y., Davis, R. E., Wiestner, A., Alizadeh, A. A., Arthur, D. C., Mitchell, J. B., Marti, G. E., Fowler, D. H., Wilson, W. H., Staudt, L. M. (2004) Fludarabine treatment of patients with chronic lymphocytic leukemia induces a p53-dependent gene expression response. *Blood* **104,** 1428–1434.
29. Townsend, P. A., Cragg, M. S., Davidson, S. M., McCormick, J., Barry, S., Lawrence, K. M., Knight, R. A., Hubank, M., Chen, P. L., Latchman, D. S., Stephanou, A. (2005) STAT-1 facilitates the ATM activated checkpoint pathway following DNA damage. *J. Cell Sci.* **118,** 1629–1639.
30. Townsend, K. P., Shytle, D. R., Bai, Y., San, N., Zeng, J., Freeman, M., Mori, T., Fernandez, F., Morgan, D., Sanberg, P., Tan, J. (2004) Lovastatin modulation of microglial activation via suppression of functional CD40 expression. *J. Neurosci. Res.* **78,** 167–176.
31. Dupuis, S., Jouanguy, E., Al-Hajjar, S., Fieschi, C., Al-Mohsen, I. Z., Al-Jumaah, S., Yang, K., Chapgier, A., Eidenschenk, C., Eid, P., Al Ghonaium, A., Tufenkeji, H., Frayha, H., Al-Gazlan, S., Al-Rayes, H., Schreiber, R. D., Gresser, I., Casanova, J. L. (2003) Impaired response to interferon-α/β and lethal viral disease in human STAT1 deficiency. *Nat. Genet.* **33,** 388–391.
32. Nimmerjahn, F., Dudziak, D., Dirmeier, U., Hobom, G., Riedel, A., Schlee, M., Staudt, L. M., Rosenwald, A., Behrends, U., Bornkamm, G. W., Mautner, J. (2004) Active NF-κB signaling is a prerequisite for influenza virus infection. *J. Gen. Virol.* **85,** 2347–2356.
33. Smiley, S. T., Reers, M., Mottola-Hartshorn, C., Lin, M., Chen, A., Smith, T. W., Steele Jr., G. D., Chen, L. B. (1991) Intracellular heterogeneity in mitochondrial membrane potentials revealed by a J-aggregate-forming lipophilic cation JC-1. *Proc. Natl. Acad. Sci. USA* **88,** 3671–3675.
34. Reers, M., Smith, T. W., Chen, L. B. (1991) J-aggregate formation of a carbocyanine as a quantitative fluorescent indicator of membrane potential. *Biochemistry* **30,** 4480–4486.
35. Fagard, R., Mouas, H., Dusanter-Fourt, I., Devillers, C., Bissieres, P., Martin, A., Lenoir, G., VanTan, H., Feuillard, J., Raphael, M. (2002) Resistance to fludarabine-induced apoptosis in Epstein-Barr virus infected B cells. *Oncogene* **21,** 4473–4480.
36. Nepomuceno, R. R., Snow, A. L., Robert Beatty, P., Krams, S. M., Martinez, O. M. (2002) Constitutive activation of Jak/STAT proteins in Epstein-Barr virus-infected B-cell lines from patients with posttransplant lymphoproliferative disorder. *Transplantation* **74,** 396–402.
37. Najjar, I., Baran-Marszak, F., Le Clorennec, C., Laguillier, C., Schischmanoff, O., Youlyouz-Marfak, I., Schlee, M., Bornkamm, G. W., Raphaël, M., Feuillard, J., Fagard, R. (2005) Latent membrane protein 1 regulates STAT1 through NF-κB-dependent interferon secretion in Epstein-Barr virus-immortalized B cells. *J. Virol.* **79,** 4936–4943.
38. Schwartz, J. L., Jordan, R., Evans, H. H., Lenarczyk, M., Liber, H. (2003) The TP53 dependence of radiation-induced chromosome instability in human lymphoblastoid cells. *Radiat. Res.* **159,** 730–736.
39. Alvi, A. J., Austen, B., Weston, V. J., Fegan, C., MacCallum, D., Gianella-Borradori, A., Lane, D. P., Hubank, M., Powell, J. E., Wei, W., Taylor, A. M., Moss, P. A., Stankovic, T. (2005) A novel CDK inhibitor, CYC202 (R-roscovitine), overcomes the defect in p53-dependent apoptosis in B-CLL by down-regulation of genes involved in transcription regulation and survival. *Blood* **105,** 4484–4491.
40. Townsend, P. A., Scarabelli, T. M., Davidson, S. M., Knight, R. A., Latchman, D. S., Stephanou, A. (2004) STAT-1 interacts with p53 to enhance DNA damage-induced apoptosis. *J. Biol. Chem.* **279,** 5811–5820.
41. Siliciano, J. D., Canman, C. E., Taya, Y., Sakaguchi, K., Appella, E., Kastan, M. B. (1997) DNA damage induces phosphorylation of the amino terminus of p53. *Genes Dev.* **11,** 3471–3481.
42. Chapgier, A., Wynn, R. F., Jouanguy, E., Filipe-Santos, O., Zhang, S., Feinberg, J., Hawkins, K., Casanova, J. L., Arkwright, P. D. (2006) Human complete Stat-1 deficiency is associated with defective type I and II IFN responses in vitro but immunity to some low virulence viruses in vivo. *J. Immunol.* **176,** 5078–5083.
43. Ohmori, Y., Hamilton, T. A. (1997) IL-4-induced STAT6 suppresses IFN-γ-stimulated STAT1-dependent transcription in mouse macrophages. *J. Immunol.* **159,** 5474–5482.
44. Look, D. C., Pelletier, M. R., Tidwell, R. M., Roswit, W. T., Holtzman, M. J. (1995) Stat1 depends on transcriptional synergy with Sp1. *J. Biol. Chem.* **270,** 30264–30267.
45. Stewart, M. D., Choi, Y., Johnson, G. A., Yu-Lee, L. Y., Bazer, F. W., Spencer, T. E. (2002) Roles of Stat1, Stat2, and interferon regulatory factor-9 (IRF-9) in interferon τ regulation of IRF-1. *Biol. Reprod.* **66,** 393–400.